Impression creep testing across a heat affected zone

J.H. Rantala [1]*, T. Andersson [1]

[1] VTT Technical Research Centre of Finland Ltd

* Correspondence: juhani.rantala@vtt.fi; Tel.: +358400570386

Abstract: Impression creep testing was applied for studying the creep strain rates in the heat affected zone of a P22 weld in order to support an FE analysis of a piping system. The specimen size recommendations for impression creep were violated in the sense that instead of a standard 10*10*2.5mm specimen an oversize 10*10*10 mm specimen was machined such that the heat affected zone was in the middle of the specimen. By grinding the specimen after each test cycle, the material combination from the base material through the HAZ to the weld metal was "scanned" as the specimen got thinner. The validity of the measured strain rates is supported by FE analysis, which showed that the creep deformation is very strongly concentrated in the immediate vicinity of the indenter while the underlying material remains unaffected. The effect of the previous loading was removed by grinding off the top layer. The strain rate distribution and primary strain component distribution vs. distance from the fusion line were determined. These results were applied in the FE analysis of full size piping components.

Keywords: impression creep, heat affected zone, FE analysis, stress analysis, piping

1. Introduction

In creep stress analysis of a live steam piping accurate material creep properties are needed. These can be obtained by traditional creep testing. However, for a detailed analysis of welded steam piping components also the properties of the heat affected zone would be needed. Uniaxial cross-weld testing would be useful, but the testing will not give the creep properties of the individual zones within the heat affected zone. Therefore, Impression Creep testing was applied in a research project [1] lead by Inspecta Technology, Sweden, and funded by Energiforsk AB (formerly Värmeforsk). By using an oversize specimen, it was possible to scan through the whole weldment from weld metal, across the heat affected zone, and to the base metal. In this way the creep properties of the heat affected zone were measured and implemented into an FE code, from this the critical locations in the piping system can be analysed in a more reliable manner.

2. Materials and Methods

Virgin 10CrMo910 (P22) tube 273*32mm was welded and post weld heat treated according to the welding procedure of the power plant Heleneholmsverket in Malmö, Sweden by using a matching consumable, TIG welding, preheat temperature 150-200°C, interpass temperature 350°C, PWHT 1h at 680-720°C. Samples were removed for uniaxial and Impression Creep testing as shown in Figure 1. From the weld cross-section an oversize 10*10*10mm Impression Creep "sandwich" specimen was removed as shown in Figure 2. The HAZ was parallel with the surface to be indented. The specimen was deliberately thicker than the recommended standard 2.5mm thick specimen to facilitate scanning of different material constituents within a specimen by grinding off 0.5mm after each test cycle and continuing with a fresh surface. By using an oversize specimen, it was assumed that the extra thickness would cause only minor error and most of the creep deformation of the previous test cycle is removed by grinding. The specimen was rotated by 90° after each test cycle, which also reduces the effect of the deformation under the indenter from the previous cycle.

Figure 1. Welded 10CrMo910 pipe (273*32mm) after removal of test specimens.
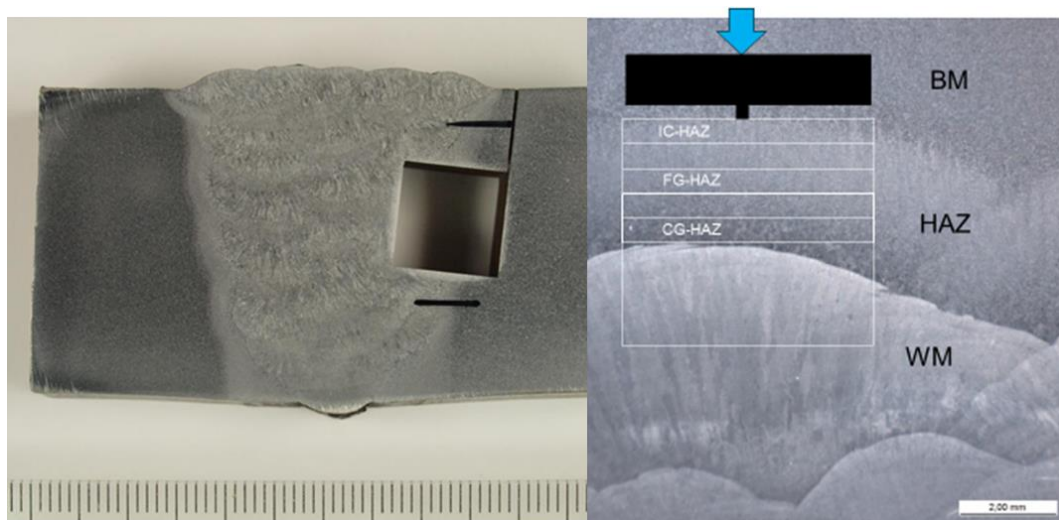
Figure 2. Left: Cross-section and the locations of the impression creep specimens and the hardness measurements across the HAZ (black lines), mm-scale at the bottom, right: schematic of the loading arrangement through different constituent of the weldment.

3. Results

The typical duration of an Impression Creep test is 500h. After each test cycle the minimum displacement rate was calculated and this was converted to a corresponding uniaxial strain rate by using a simple analytical equation established for Impression Creep to uniaxial conversion [2]. Also, the displacement curves (indentation depth) were converted to uniaxial strain curves as shown in Figure 3 where the curves of the nine first tests are shown. The continuous strain rate curves shown in Figure 4 were calculated by moving a 100 h "calculation window" from the beginning of the test to the end. It is seen that towards the end of each test the scatter increases when the strain rates become very small. In another project it was defined that below a strain rate of about $3*10^{-6}$ the accuracy will reduce [3]. This is also partly because towards the end of the test, the number of data points in the 100 h calculation window reduces and in fact, the last rate is calculated by a window of only 50 h. A linear trend line was fitted through the data of the last 100h of each test in order to calculate the corresponding uniaxial minimum creep rate of each test according to the standard conversion equation. By doing this, it was assumed that the reducing specimen thickness does not cause much error in the conversion calculation. To verify this a detailed FE analysis would be needed. The Impression Creep tests in this study were carried out at 530°C and an equivalent stress of 110 MPa. The measured creep rates are shown in Table 1.
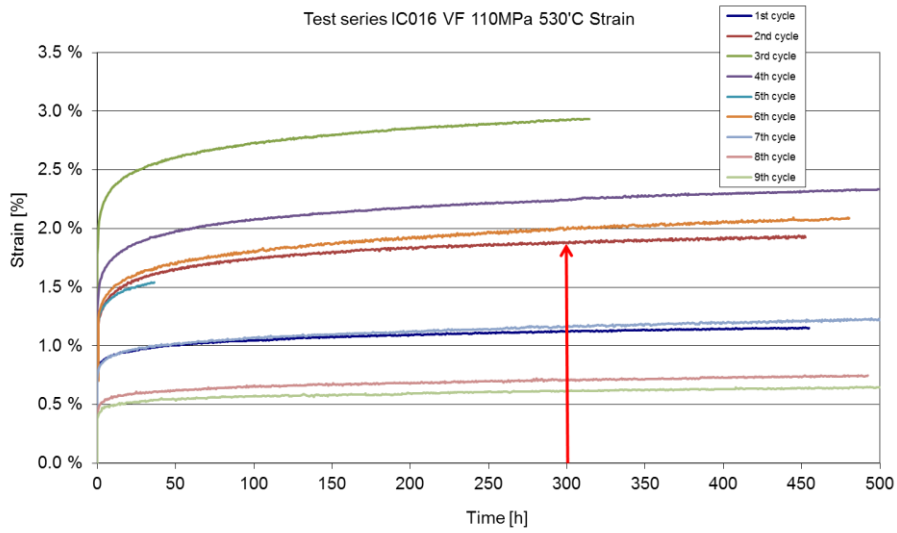
Figure 3. Corresponding uniaxial strain curves calculated from the Impression Creep test series at 110 MPa and 530°C.
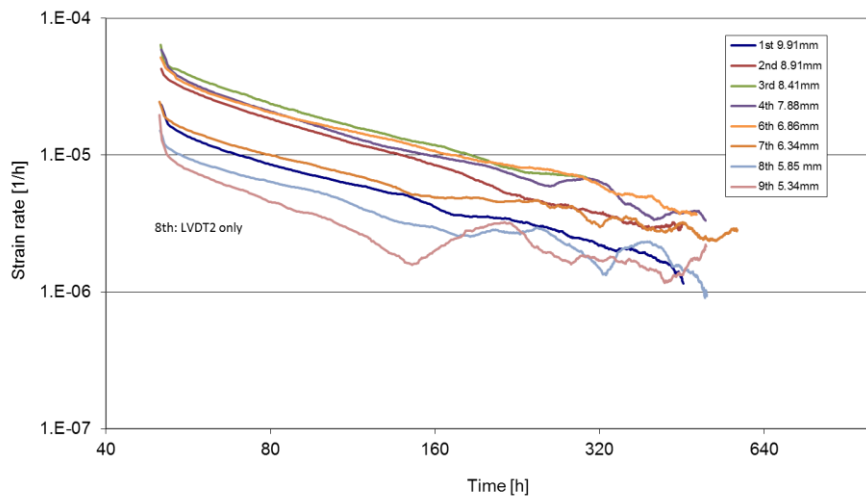
Figure 4. Continuous strain rate curves from the Impression Creep test data in Figure 3.

Table 1. Minimum linear strain rates at each specimen thickness at 110 MPa 530°C.

Specimen thickness [mm]	min. strain rate (corrected) [1/h]
9.91	1.75E-06
8.91	3.26E-06
8.41	3.90E-06
7.88	3.70E-06
6.86	4.58E-06
6.34	2.74E-06
5.85	1.65E-06
5.34	1.44E-06
4.85	1.79E-06
3.88	1.22E-06
3.09	9.47E-07
2.5	5.29E-07

The creep rate varied when moving from BM across the HAZ to the WM. The useful illustration of this behaviour is shown in Figure where the brown curve shows the corresponding uniaxial strain at a constant time value of 300 h, being a rough relative measure of the amount of primary creep at each material layer. However, the quality of the initial contact between the specimen and the indenter is not necessarily perfect in each test, so there is some uncertainly associated with this strain parameter. However, the strain value (brown curve) and the calculated minimum creep rate (blue curve) for each test seem to go roughly hand in hand. Standard deviation values were added on the strain rate curve as calculated at the same time period as the minimum strain rate.

The test series was started with the specimen thickness of 10 mm and at that thickness the tested surface was in base material. After the first test 1 mm was ground off and in the second test the measured minimum strain rate increased. After the following tests only 0.5 mm was ground off. However, two tests (at thicknesses 8.41mm and 4.85mm) were run to only about 300h instead of intended 500h test duration. Based on the general trend in Figure 4 it was estimated that the creep rate at 500h would be 0.54 times the rate at 300h. When these two test results are corrected, the maximum strain rate appears at a location which is likely to be the inter-critical (partially austenitized) zone, see Figure 5.

Based on the measurements from the cross-section of the weld in Figure 2 it can be estimated that on top of the 10*10mm hole the location of the fusion line is at 3.7 mm and at the bottom at 5.1 mm. The location of the IC-HAZ/BM transition is more difficult to define but is located roughly at 6.3 mm on top of the hole and at 7.0 mm at the bottom. The red inclined lines in Figure 5 illustrate the locations of the HAZ constituents on two opposite side of the specimen. From these measurements it can be estimated that the width of the HAZ is 2.6 mm on top of the hole and 1.9 mm at the bottom, which seem like rather small values. The CG-HAZ is the strongest zone and has the lowest creep rate. The minimum creep rate results in Table 1 and in Figure 5 show that the highest strain rate of $4.58*10^{-6}$ is only about 2.6 times higher than in the base material ($1.75*10{-6}$). However, it was expected that the strain rate in the coarse-grained zone would have been considerably lower than in the base material, but this is not the case. The low creep rates measured from the WM as shown in Figure 5 indicate that the creep strength of the WM is slightly higher than of the BM. The weld is therefore overmatching.

The reported minimum strain rate values did not necessarily hit the lowest (intercritical zone) or the highest (coarse grained zone) values in the test specimen because the fusion line in a real weld is not straight and therefore the material under the indenter is not likely to contain just one thin layer of each constituent of the HAZ. Besides that, the selected grinding thickness of 0.5 mm was a compromise between two factors. First, the smaller the grinding thickness, the smoother the curve in Figure5 would have been (but would have increased the number of test cycles needed to scan through the specimen). Secondly, the smaller the grinding thickness, the more the deformation from the previous cycle would have influenced the following test. The FE analysis of the IC test specimen has shown that only very little deformation below the indenter will progress deeper than 0.5 mm. However, this is of course dependent on the stress level as shown in section 4.

When testing a HAZ specimen as described above it must be recognised that the sample is a sandwich structure in terms of material properties. At this point it is not known how the underlying different microstructures will affect the testing of the microstructure on the surface. This would require FE analysis which was not foreseen in the Energiforsk project.
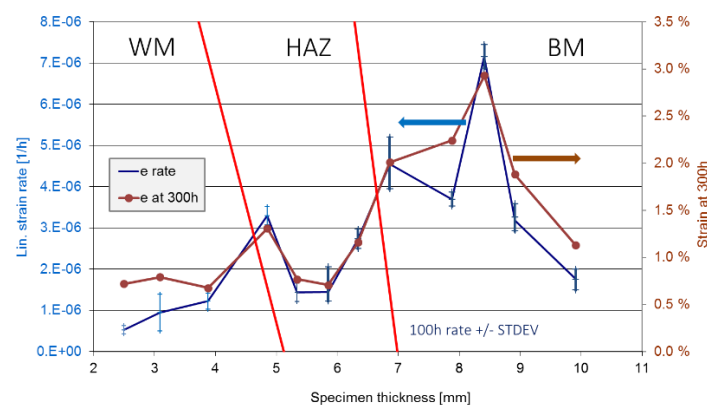
Figure 5. Calculated minimum linear strain rate (with error bars) and the corresponding uniaxial strain at 300 h for each impression creep test at 110 MPa and 530°C.

3.1. Hardness measurement

Hardness was measured from the new weld and the results are shown in Figure 6. The locations of the hardness measurements are indicated in Figure 2. The hardness measurements suggest that the width of the HAZ is about 4 mm, which does completely coincide with the measurements taken from the specimen itself. The WM has much higher hardness (250 HV1) than the BM (160 HV1), which means that the WM is overmatching. The high hardness of the WM is in line with the finding that the creep rate of the WM in Figure 5 is lower than the creep rate of the BM although the correlation between hardness and creep strength is in most cases only coincidental.
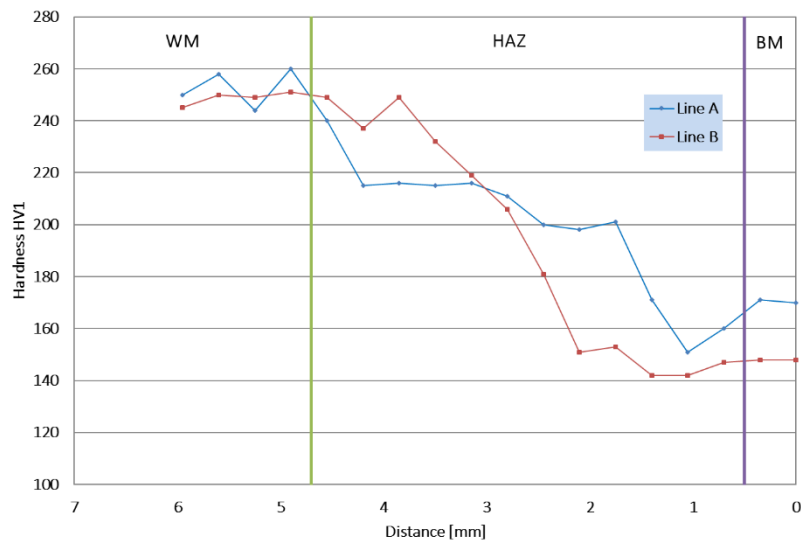
Figure 6. Hardness measurements across the HAZ of the weld.

4. FE analysis of impression creep test

The impression creep test was analysed by the FE method with Abaqus CAE software (version 6.14). A quarter model of the impression creep test for the 2.5mm thick standard specimen was used. For the 10mm thick specimen a different mesh was used. Specimens were meshed with 62500 and 48000 quadratic elements (C3D20R), respectively.

The LCSP creep model [4] for 10CrMo910 was used at 525°C with a contact pressure of 255.8 MPa, which corresponds to a uniaxial stress of 110 MPa, which was used in the IC test programme. The temperature of 525°C was used in the analysis instead of the real test temperature of 530°C, because the parametric LCSP model did not converge properly, but the LCSP model trimmed for 525°C was available and worked nicely. This difference in temperature leads to an error of less than 10% in strain rate.

The plots of the equivalent strain in Figure 7 and Figure 8 show that the maximum strain is located a short distance below the indenter edge and about 0.5mm below the indenter in the middle. This means that when 0.5mm of the 10mm thick specimen was ground after each test cycle, some strain (less than 0.08%) from the previous test was left on the surface of the ground specimen in the area directly under the indenter. The effect of this was however minimised by turning the specimen 90° along the vertical axis. After turning the specimen about 90% of the surface under the indenter is practically unstrained.

The strain distribution in the 10mm thick specimen in Figure 9 is rather similar to the 2.5mm thick specimen, but the strain in the thick specimen seems to spread deeper than in the standard specimen.
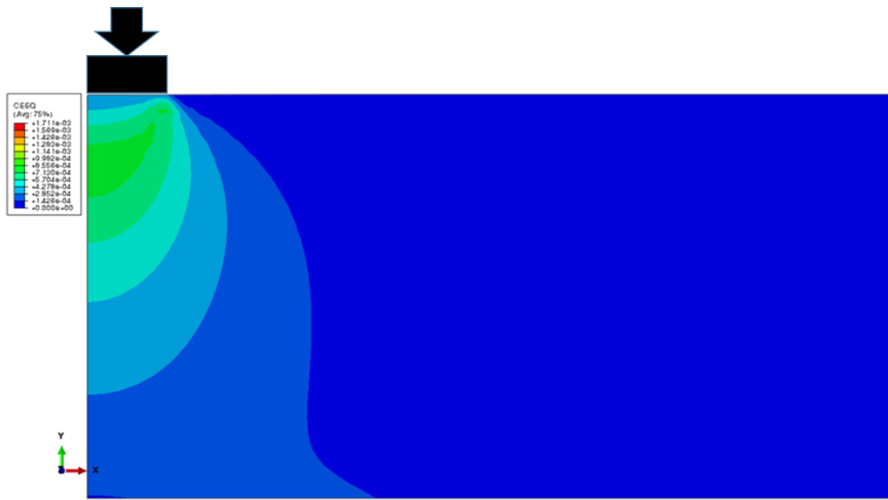
Figure 7. Half model of the equivalent strain distribution in the 2.5mm thick specimen.
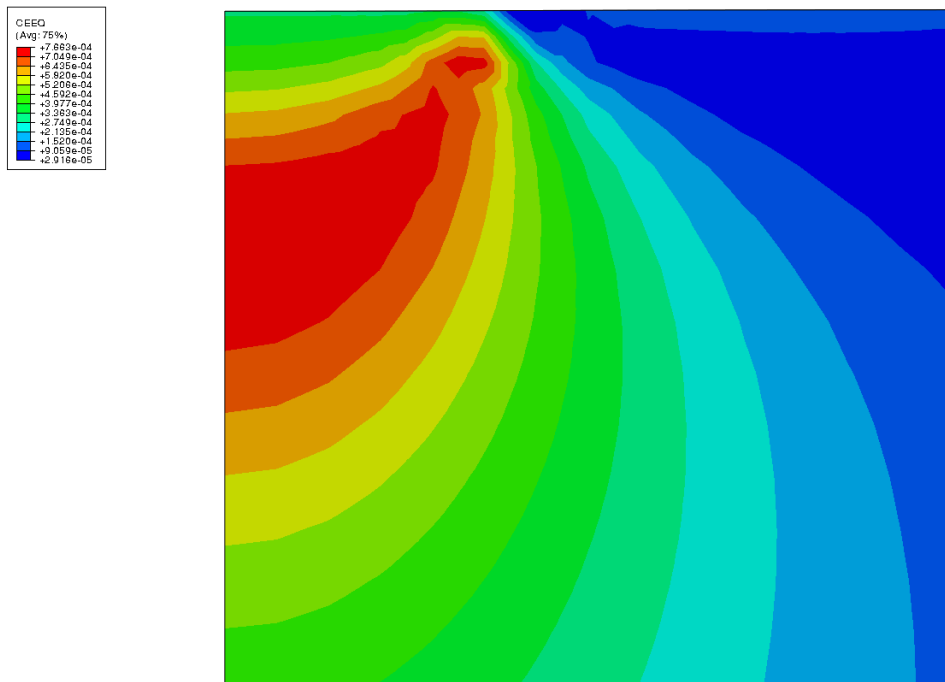
Figure 8. Close-up of Fig. 18 (1.4*1.3mm).
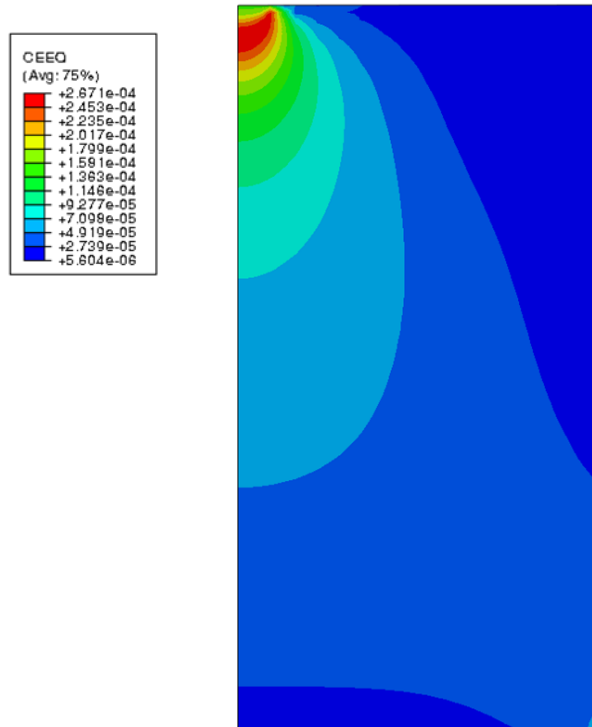
Figure 9. The equivalent strain distribution in the 10mm thick specimen.

The displacement as a function of time was predicted by the FE analysis. The initial strain in the 10mm thick specimen was bigger by a factor of 1.84 than in the standard specimen, but the strain rate at 500 h in the 10mm specimen was 30% smaller than in the standard specimen. The expectation was that making the specimen thicker would not make much difference in the behaviour, because most of the strain should be concentrated just below the indenter. As shown in Figure 9, the strain level at the bottom of the thick specimen is small but sufficient to have an effect on the total strain and strain rate levels. When compared to the experimental strain rate measurements with the 10mm thick specimen, the FE predictions fell short by a factor of 5.

5. Conclusions

An innovative way of applying impression creep testing was used by manufacturing a "sandwich" type of specimen of a welded joint, which allowed the creep rates to be scanned from the base material across the HAZ to the weld metal. The highest creep rate in the inter-critical zone of the welded joint was, however, not as high as was expected: only 2.6 times higher than in the base material. The weld metal is slightly overmatching as compared to the base material. The measured HAZ creep rates were entered as part of material property data for the FE analysis of a live steam piping system and its components.

References

1. Storesund, J.; Steingrimsdottir, K.; Rantala, J.; Sollander, R.; Chen, Z.; Bolinder, T. Lifetime assessment of high temperature piping by stress analysis and testing, Report M12-218, Energiforsk AB, 2015.
2. Hyde, T.H.; Sun, W.; Brett, S.J. Some Recommendations on the Standardization of Impression Creep Testing, ECCC Creep Conference, 21–23 April 2009, Zurich.
3. Brett, S.J.; Rantala, J.H.; Holmström, S. Practical application of impression creep data to power plant, in proceedings of Baltica IX, Intl. Conf. on Life Management and Maintenance for Power Plants, 11-13 June 2013, Eds. Auerkari, P.; Veivo, J. Helsinki-Stockholm-Helsinki, 2013.
4. Holmström, S. Engineering tools for robust creep modeling. Doctor's dissertation, Aalto University, Espoo, 5 Febr. 2010. VTT, Publication 728 (2010), VTT, Espoo, 94 + 53 p, ISBN 978-951-38-7378-3.